Hindawi Publishing Corporation
Science and Technology of Nuclear Installations
Volume 2015, Article ID 620205, 11 pages
http://dx.doi.org/10.1155/2015/620205

Research Article

Study of the Reactor Control System of MSHIM in AP1000

Xinyu Wei and Fuyu Zhao

School of Energy and Power Engineering, Xi'an Jiaotong University, Xi'an, Shaanxi 710049, China

Correspondence should be addressed to Xinyu Wei; xyu.wei@yahoo.com

Received 8 September 2015; Revised 4 November 2015; Accepted 12 November 2015

Academic Editor: Eugenijus Uščpuras

According to the mechanism analysis and simulation of power control system of MSHIM in AP1000, a modified MSHIM (Mechanical Shim) control strategy is presented, which employs the error between the reactor coolant average temperature and its reference value as the unique control signal with a P-controller added. The modified MSHIM control strategy is verified by simulations of three typical working conditions. The results show that the modified power control system satisfies the needs of reactor core power control and power distribution control. The conclusions have reference value for the engineering practice.

1. Introduction

AP1000 is a two-loop pressurized water reactor (PWR) developed by Westinghouse, which uses the forces of nature and simplicity of design to enhance plant safety and reduce construction costs [1]. It received Final Design Approval by the United States Nuclear Regulatory Commission (NRC) in 2004 and Design Certification by USNRC in 2005 [2]. In China, the AP1000 has become one of the best candidates for the next generation of nuclear power plants due to its passive safety features and economic competitive power.

Compared to traditional reactor control strategies, the AP1000 adopts a different core control strategy, called Mechanical Shim (MSHIM) [3]. The MSHIM contains two independent sets of control systems, the core power control system and the axial power distribution control system. The core power control system uses the gray and black M control banks (M-banks) for power level control; however, the axial power distribution control system uses the axial offset (AO) control bank (AO-bank) for axial power distribution control. In traditional PWRs, the same control bank is used for both power control and axial power distribution control, which can easily cause high variation in local power distributions and incline for xenon transients. In addition, existing PWRs use the control rod movement supplemented by adjustments of the soluble boron concentration in the moderator during power maneuvers, while, in AP1000, the power change operations can be totally automated with the MSHIM control strategy without boron concentration adjustments, which can reduce the daily effluent to be disposed.

When it comes to the power control system, a three-channel controller is adopted in MSHIM, which is disposed from the traditional PWRs control system. In MSHIM control system, the AO control system is mainly reformed, but the power control system is similar to that in traditional PWR's control system. Many scholars have been studying the control system of AP1000 and mainly focus on (1) studies on implementation of the MSHIM control strategy, (2) transient simulation and analysis of the whole nuclear power plant, and (3) the MSHIM control strategy application in traditional PWRs. Onoue et al. [4] studied the application of MSHIM control strategy for AP1000 nuclear power plant using the quasistatic program. Drudy et al. [5] analyzed the robustness of the MSHIM control strategy using the program of the Westinghouse. Fetterman [6] simulated and analyzed the base load and day load follow operation of AP1000 nuclear power plant by PHONEIX-P and ANC. Liu et al. [7] simulated the control system and protection system of AP1000 nuclear power plant using RELAP5; their study verified the whole plant control system, including MSHIM control system, under the representative operational transient. All these researches focused on the application, simulation, and verification of the MSHIM, but few of them regarded the power control system in MSHIM.

As far as we know, the studies on the power control system in the MSHIM are very scarce. The present study aims at this

purpose. This paper shows two main contributions of our work. Firstly, according to the simulation and analyzing of the original MSHIM control strategy, the power control system in MSHIM is modified. Secondly, the modified power control system is verified by three representative transient conditions.

The remaining of this paper is organized as follows. Section 2 introduces the simulation platform of control system in AP1000. Section 3 presents a modified power control system of MSHIM, after the simulation and analyzing of the original control system. The modified control strategy is simulated and verified in Section 4, and the simulation results are discussed. Finally, conclusion is given in Section 5.

2. Simulation Platform

In this paper, a simulation platform called Reactor Core Fast Simulation Program (RCFSP), which is developed in the MATLAB/SIMULINK environment based on the nodal method, is used for simulation and verification of the original and improved control strategy [8].

2.1. Nodal Core Model. For detailed models containing the core physics calculations, thermal-hydraulic analysis and burnup optimization are too costly for the dynamic simulations of the nuclear reactor because they are very complex and need tremendous calculation work. Therefore, a nodal method is used to describe the global power and axial power distribution of AP1000 reactor core here. The nodes are treated as independent cores coupled with each other through neutron flux. It is assumed that the neutron flux and material composition in each node are uniform. Thus, the neutron flux and other neutronic parameters in each node are represented by the respective average values integrated over its volume [9].

Figure 1 shows the nodalization and neutron diffusion of nodal reactor model schematically. Since the nodal method can describe the space-time neutron kinetics simply and effectively, it is adopted for the modeling and simulation of AP1000 in RCFSP. And then, the AP1000 reactor core is divided into 14 nodes in the axial direction [10].

As described before, the nodal core model contains the neutron kinetic equations as (1) and (2), heat transfer equations as (3) and (4), idiom and xenon kinetic equations as (5) and (6), and reactivity equations as (7). Therefore,

$$\frac{dN_i}{dt} = \left(\frac{\rho_i - \beta}{\Lambda_i} - \frac{D_i \nu}{\Delta H_i d_{i,i-1}} - \frac{D_i \nu}{\Delta H_i d_{i,i+1}}\right) N_i + \sum_{k=1}^{6} \frac{\beta_k}{\Lambda_i} C_{k,i} + \frac{D_i \nu n_{i-1}(0)}{\Delta H_i d_{i,i-1} n_i(0)} N_{i-1} + \frac{D_i \nu n_{i+1}(0)}{\Delta H_i d_{i,i+1} n_i(0)} N_{i+1}, \quad (N_0 = 0,\ N_{14} = 0), \tag{1}$$

$$\frac{dC_{k,i}}{dt} = \lambda_k \left(N_i - C_{k,i}\right), \quad k = 1, 2, \ldots, 6,\ i = 1, 2, \ldots, n, \tag{2}$$

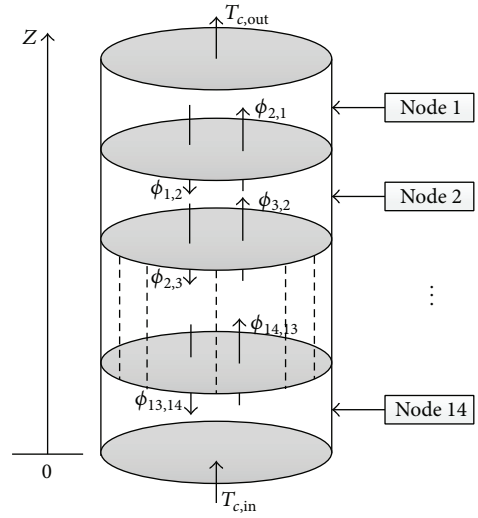

Figure 1: Nodalization of the AP1000 reactor core in the axial direction.

$$\frac{dT_{fi}}{dt} = \frac{f_f P_{i0}}{\mu_{fi}} N_i - \frac{\Omega_i}{\mu_{fi}} T_{fi} + \frac{\Omega_i}{\mu_{fi}} T_{\text{ci}}, \tag{3}$$

$$\frac{dT_{\text{ci}}}{dt} = \frac{\left(1 - f_f\right) P_{i0}}{\mu_{\text{ci}}} N_i + \frac{\Omega_i}{\mu_{\text{ci}}} T_{fi} - \frac{\Omega_i + 2M_i}{\mu_{\text{ci}}} T_{\text{ci}} + \frac{2M_i}{\mu_{\text{ci}}} T_{\text{ci,in}}, \tag{4}$$

$$\frac{dI_i}{dt} = \lambda_I \left(N_i - I_i\right), \tag{5}$$

$$\frac{dX_i}{dt} = \frac{\lambda_X + \sigma_{a,i}^X \phi_{i0}}{\gamma_I - \gamma_X} \left(\gamma_X N_i + \gamma_I I_i\right) - \left(\lambda_X + \sigma_{a,i}^X \phi_{i0} N_i\right) X_i, \tag{6}$$

$$\rho_i = \rho_{ri} + \alpha_{fi} \left(T_{fi} - T_{fi,0}\right) + \alpha_{\text{ci}} \left(T_{\text{ci}} - T_{\text{ci},0}\right) + \alpha_{Xi} \left(X_i - X_{i0}\right) + \rho_{i0}, \tag{7}$$

where subscript i has been used to denote the ith node, n is the number of nodes in the reactor, the reactor core is divided into 14 nodes in the axial direction here, so $n = 14$, N and C_k denote the relative neutron concentration and the relative concentration of the kth delayed neutron precursor, respectively, $N_0 = 0$, $N_{14} = 0$, β_k is the fraction of the kth delayed neutron group, λ_k is the decay constant of the kth delayed neutron precursors, D denotes the diffusion coefficient, Λ denotes the average neutron generation time, ΔH_i is the height of the ith node, $d_{i,i-1}$ and $d_{i,i+1}$ are the distances between the centers of the ith node and its neighboring nodes, $n_i(0)$ and P_{i0} are the neutron concentration at rated power level and the rated reactor thermal power for the ith node, respectively, f_f is the fraction of the core power generated in the fuel, T_f and T_c denote the average temperatures of fuel and coolant, respectively, $T_{\text{ci,in}}$ is the coolant inlet temperature inside the ith node, Ω denotes the transfer

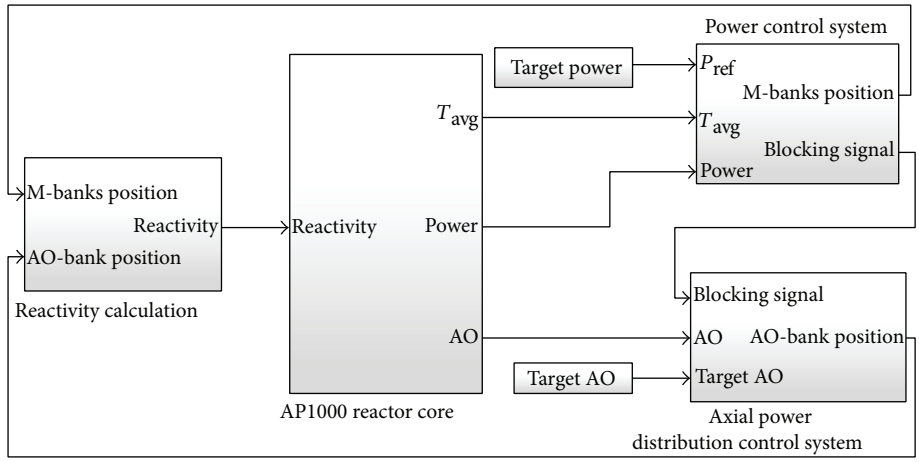

Figure 2: RCFSP, simulation platform of AP1000 in MATLAB/SIMULINK environment.

coefficient between the fuel and coolant, μ_f and μ_c denote the total heat capacities of the fuel and coolant, respectively, M denotes the product of mass flow rate and the heat capacity of the coolant, I and X denote the relative concentrations of iodine and xenon, respectively, ϕ_{i0} and $\sigma_{a,i}^{X}$ are the neutron flux at rated power level and the microscopic cross section for absorption for the xenon inside the ith node, respectively, γ_I and γ_X are the fission yields of iodine and xenon, respectively, λ_I and λ_X are, respectively, the decay constants of iodine and xenon, ρ_r denotes the reactivity contributed by control rods, α_f, α_c, and α_X denote the reactivity coefficients of the fuel, coolant, and xenon, respectively, $T_{fi,0}$ and $T_{ci,0}$ are the steady-state values of the fuel and coolant average temperatures inside the ith node, respectively, X_{i0} is the steady-state value of the relative xenon concentration inside the ith node, and ρ_{i0} is the initial reactivity inside the ith node.

2.2. Reactor Core Fast Simulation Program. The simulation flow diagram of RCFSP in SIMULINK is shown in Figure 2.

The RCFSP is mainly made up of five parts: the power demand part, the M-banks control system for power control, the AO-bank control system for axial power control, the reactivity calculation part, and the reactor core. The power demand part provides the target power for MSHIM operations. The M-banks control system accounts for the core reactivity changes due to changes in power level and xenon concentration by the M-banks position adjustment. The AO-bank control system maintains the core thermal margin within operating and safety limits through the motion of AO-bank. The motion of control rods would cause a change in the reactivity introduced into the reactor core. The reactor core calculates the variations of main physical and thermal-hydraulic parameters with the variable step size solver Ode15s.

The simulation process of RCFSP is described in Figure 3. As illustrated in Figure 3, the necessary variables at the steady-state conditions are obtained before performing dynamic simulations. And then, three iterations will circulate until the simulation period as in Figure 3.

This simulation platform is developed in MATLAB/SIMULINK version R2014a. And this study is performed in a PC with CPU 2.30 GHz, ROM 8 GB, and Windows 8.1 operating system.

3. Modified Power Control System in MSHIM

For nuclear reactor cores, the function of the power control system is to control and balance the core power and the load of turbine. Usually, the power control system is also referred to as the reactor coolant average temperature control system, whose function is implemented based on the three-channel nonlinear controller, as shown in Figure 4.

From Figure 4, it is clear that two control input signals contribute to the motion of the M-banks. The error between coolant average temperature (T_{avg}) and the programmed reference coolant average temperature (T_{ref}) constitutes the primary control signal. The value T_{ref} increases linearly with turbine load from the zero-power to the full-power condition. Another control input signal is derived from the reactor power versus turbine load mismatch signal, which improves system performance by enhancing response and reducing transient peaks. To reduce the total control rod movement and subsequent wear on the control rods, a dead band is included in the power control subsystem so that no rod motion is demanded if the T_{avg} error is within the dead band. As the T_{avg} error increases, the rod speed becomes greater. For power control, the rod speed demand signals of the M-banks vary over the range of 8 to 72 steps/min. This variable-speed drive provides the ability to insert small amounts of reactivity at low speeds to give fine control of T_{avg} as well as to furnish control at high speeds to correct larger temperature transients.

As shown in Figure 4, the T_{avg} signal passes a compensation circuit including the following components:

$$G_1 = \frac{1}{1+\tau_1 s},$$
$$G_2 = \frac{1+\tau_2 s}{1+\tau_3 s}, \quad (8)$$

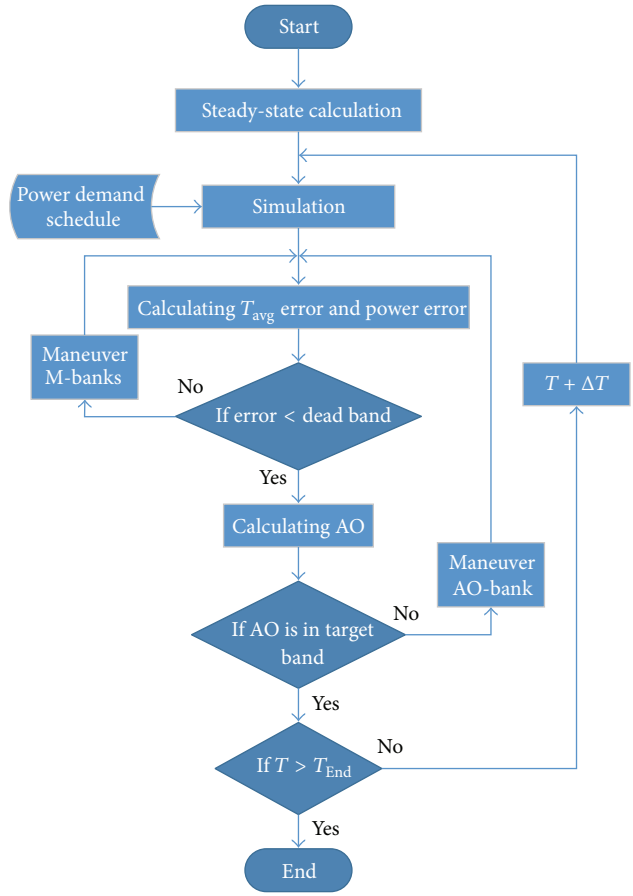

Figure 3: Simulation flow chart of RSFSP.

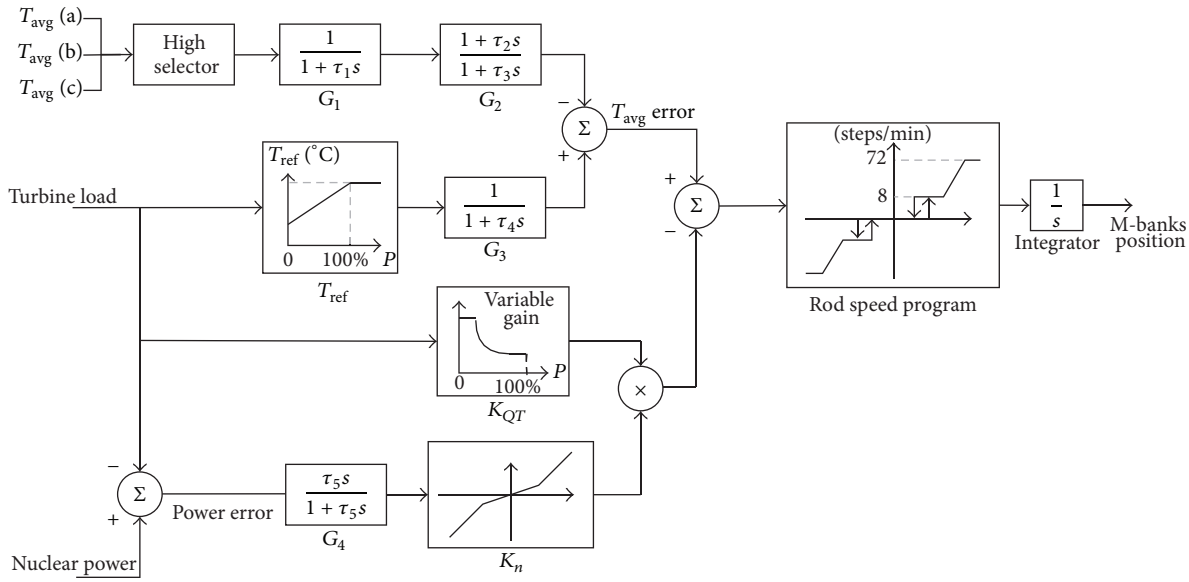

Figure 4: Block diagram of the power control system of MSHIM in AP1000.

where τ_1 is the lag time constant, τ_2 and τ_3 are the lead time constant and lag time constant, respectively, and τ_2 is larger than τ_3 here. The compensation circuit compensates for delay of response caused by the heat capacity of the temperature detector or the coolant system and makes phase-advance compensation to improve control responses. T_{ref} is set as a function of the turbine load signal (P_{ref}), which can be expressed as follows:

$$T_{\text{ref}} = \begin{cases} 291.7 + 9.2P_{\text{ref}} & 0 \le P_{\text{ref}} \le 1 \\ 300.9 & P_{\text{ref}} > 1. \end{cases} \quad (9)$$

The corresponding T_{ref} is added to the control signal after a phase lag compensation as follows:

$$G_3 = \frac{1}{1 + \tau_4 s}, \quad (10)$$

where τ_4 is the lag time constant.

The signal of power error is added to the control signal through the differential circuit, the variable gain (K_{QT}), and the nonlinear gain (K_n). The differential circuit includes the following component:

$$G_4 = \frac{\tau_5 s}{1 + \tau_5 s}, \quad (11)$$

where τ_5 is the derivative time constant. K_{QT} and K_n can be, respectively, expressed as follows:

$$K_{QT} = \begin{cases} 4 & 0 \le P_{\text{ref}} \le 0.25 \\ \dfrac{1}{P_{\text{ref}}} & 0 \le P_{\text{ref}} \le 0.25 \\ 1 & P_{\text{ref}} > 1, \end{cases} \quad (12)$$

$$K_n = \begin{cases} 0.17dP_{\text{err}} & -0.2 \le dP_{\text{err}} \le 0.2 \\ 0.83dP_{\text{err}} & dP_{\text{err}} < -0.2 \text{ or } dP_{\text{err}} > 0.2. \end{cases}$$

One of the drawbacks of using the average temperature of the coolant as the control system is that it has a significant time delay and thus introduces a large lag into the feedback loop. In this way, the power mismatch pulse should be involved to enhance the response speed of the system. However, there are some problems when the power mismatch pulse is involved. Firstly, the nuclear reactor core is a self-stabilizing system. Although the response speed of the control system can be enhanced using the power error signal, the control rods may respond too quickly in the event of a perturbation in the power signal, which reduces the efficacy of the negative feedback on the core itself. This can easily cause the loss of control rods due to fatigue. Secondly, since the time constant of the neutron kinetic equation is small, the neutron flux level is more likely to be influenced by the perturbation. Thus, the noise of the power mismatch channel is too large for its use as the differential advanced control channel. On the other hand, if a large time constant of the filter in the channel is selected, the speed and amplitude of the signal will be decreased, which is not suitable for the initial purpose of controlling in advance.

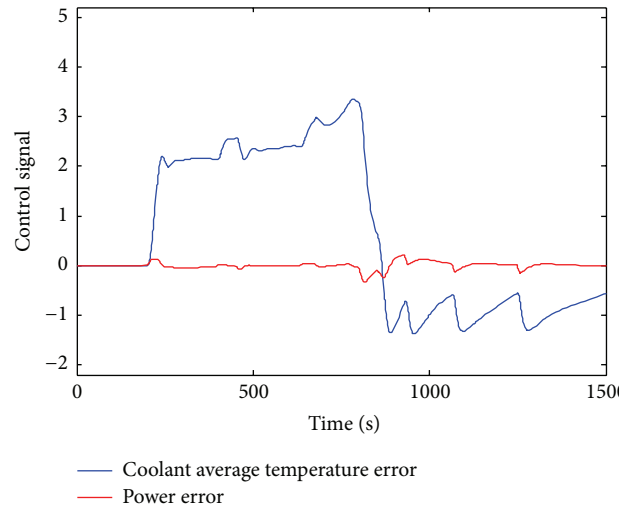

Figure 5: Comparison of two control signals under 5% FP/min ramp load decrease condition.

3.1. Error Signal Analyzing. To assess the feasibility and performance of the improved MSHIM control strategy, the original and improved MSHIM strategies are applied to AP1000 in RCFSP. The control signals of coolant average temperature error and power error are analyzed first.

AP1000 has been demonstrated to be able to perform the MSHIM operation during a wide range of anticipated operational scenarios. Among these scenarios, three typical conditions are performed in this paper.

Condition 1 (5% FP/min ramp load decrease). Power level decreases from 100% to 50% FP (full power) at a rate of 5% FP/min. The simulation duration is 1500 seconds, and, in the first 200 seconds, the reactor core is 100% FP stable. The desired power is reduced to 50% FP with a velocity of 5% FP/min from 200th second; subsequently, it is 50% FP until the end of the condition.

Condition 2 (10% FP step load decrease). Power level steps down from 100% to 90% FP. The simulation duration is 1500 seconds, and, in the first 200 seconds, the reactor core is 100% FP stable. The desired power is reduced to 90% FP at 200th second; subsequently, it is 90% FP until the end of the condition.

Condition 3 (100-50-100% FP, 12-3-6-3 h pattern of daily load follow). Power level varies from 100% to 50% in 3 h, holds at 50% for 6 h, and then rises to 100% in 3 h. The simulation duration is 96 hours, and, in the first 24 hours, the reactor core is 100% FP stable. The desired power is reduced to 50% FP from 24th hour in 3 hours, holds at 50% FP for 6 hours, and then rises to 100% FP in 3 hours; subsequently, it is 100% FP until the end of the condition.

The control signals of coolant average temperature error and power error under Conditions 1, 2, and 3 are illustrated in Figures 5, 6, and 7, respectively.

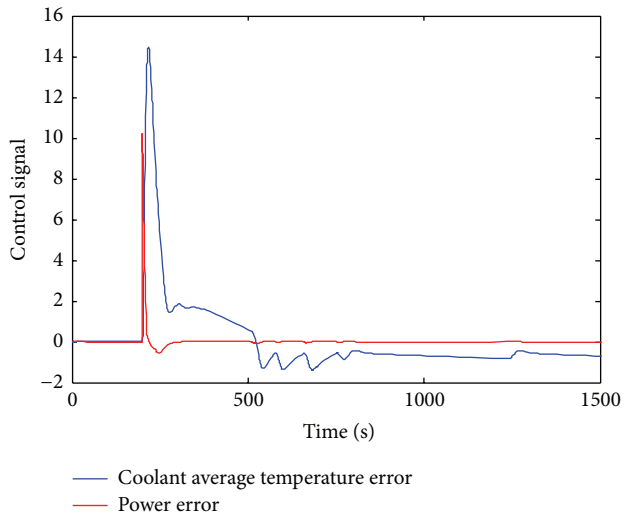

Figure 6: Comparison of two control signals under 10% FP step load decrease condition.

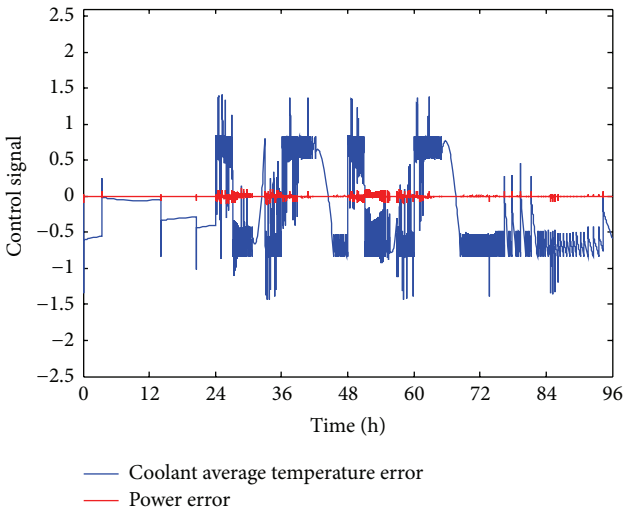

Figure 7: Comparison of two control signals under load follow condition.

Condition 1. As shown in Figure 5, compared to the coolant average temperature error signal, the value of the power error was small. To avoid the high frequent actions in the control system, a dead band of temperature of ±0.85°C was set in the M-banks system, while the nuclear power error signal was only at the level of 10-3, and its maximum amplitude is ±0.5 around the end of the ramp. Combined with the coolant average temperature error, the power error has little influence on the motion of the M-banks and hence little influence on the operation of the reactor core.

Condition 2. As shown in Figure 6, the two signals have similar tendency during this condition, but the coolant average temperature peak value is 40% more than the power error's at the beginning of the step. Furthermore, in the rest time, the power error is almost invariant compared to the coolant average temperature error. As a result, the control effect of the average temperature error signal is much greater than the power error signal and it became the dominant control signal.

Condition 3. From Figure 7, it can be seen that the coolant average temperature error is much greater than the power error. The first one's amplitude is around ±1.5, and the second one's widest value is ±0.13, which is 10% of the first one's. That means the coolant average temperature error takes a major role during the load follow condition.

From these comparisons, under three conditions, it can be seen that the power error signal is much smaller than the coolant average temperature error signal in most of conditions, and the power error signal is large within a short period of time only in the step load change condition but still smaller than the coolant average temperature error signal.

3.2. Modified Method. According to the analyzing of the control signals in the original power control system of MSHIM, a modified one is presented in this paper. Considering the smaller value of power error signal in the original system, the power error signal is eliminated. Meanwhile, for the compensation of the control speed under the step load change, a P-controller is added in the coolant average temperature error signal.

As a result, the modified power control system of MSHIM is a two-channel power controller, as shown in Figure 8. G_1, G_2, T_{ref}, and G_3 are calculated as (8)–(10), and gain of the P-controller is K_P. In the following section, the performance of the two-channel power controller will be verified.

4. Results and Discussions

4.1. Evaluation Criterion. The most important criterion to evaluate the stability of the control system is the fast and accurate control of the power level around the target value. Additionally, the AO value should be controlled within the control objective band. For quantitative analysis, 5 suitable performance indices are used to assess the performance of the original and modified MSHIM control strategies.

The squared integral of the relative power mismatch is defined as I_P:

$$I_P = \int e_P^2 \, dt, \tag{13}$$

where e_P is the difference between the relative power and the target power.

The squared integral of the AO mismatch is defined as I_{AO}:

$$I_{\text{AO}} = \int e_{\text{AO}}^2 \, dt, \tag{14}$$

where e_{AO} is the difference between the real and target AO.

The power peak factor is defined as F_z:

$$F_z = \frac{P_{\max}}{\overline{P}}, \tag{15}$$

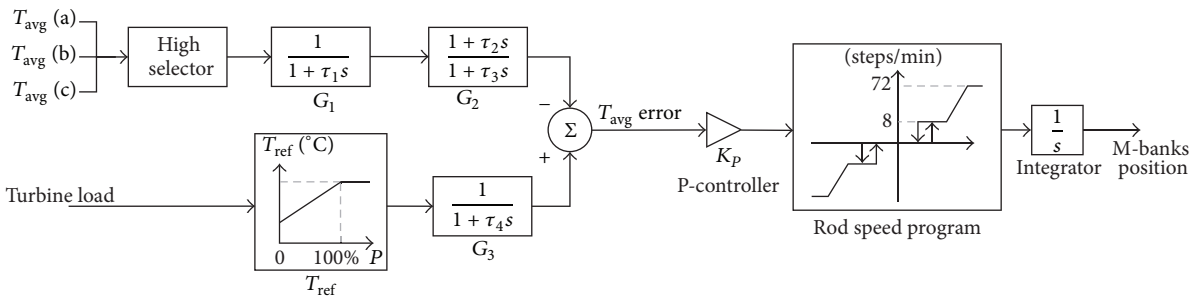

Figure 8: Modified power control system of MSHIM in AP1000.

Table 1: Parameters of the power control system simulation.

Parameters	Value
τ_1 (s)	5
τ_2 (s)	40
τ_3 (s)	5
τ_4 (s)	30
τ_5 (s)	50
K_P	2

where P_{max} is the highest power among the 14 nodes and $\overline{P}$ is the average power of the reactor core.

In addition to these three parameters, M-Steps and AO-Steps are used to show that the total steps of M-banks and AO-bank moved, respectively, are also taken into account.

I_P and I_{AO} reflect the response speed and overshooting of the system, as well as the steady-state error of the temperature and the AO mismatch. When the power and AO mismatch are larger than the nominal values, I_P and I_{AO} will be increased quadratically. The maximum power F_z^4 can be used to reflect the inhomogeneity of the four nodes, which should be as small as possible. The M-Steps and AO-Steps are used to reflect the cost when controlling the power level and distribution of the reactor core. If the motion of the control bank is smaller, the fatigue damage of the control rod driver will be smaller too.

4.2. Simulation and Analyzing. As mentioned above, three typical load change transients are simulated to assess the feasibility and performance of the original and modified control strategies. The simulation parameters are listed in Table 1. The initial positions of the control rod groups were adaptively calculated according to the model with full power.

Condition 1. The 5% FP/min ramp load decrease simulation results of the original and modified control strategy are shown in Figure 9 and Table 2.

From Figure 9, it can be seen that the reactor power follows the desired power well for both the original and modified control strategies. The overshoot of the modified strategy is smaller than that of the original one. The reason is that the modified MSHIM controls the M-banks to move faster, which can be seen in Figure 9(c). As to AO, both of the two

Table 2: Five performance indices from the 5% FP/min ramp load decrease simulation of the original and modified power control system in MSHIM.

Performance indices	I_P	I_{AO}	max F_z	M-Steps	AO-Steps
Original	196.27	5.43	1.1605	540	9
Modified	24.72	5.38	1.1602	578	9

control strategies make similar effects, but adjustment speed of AO is faster a little in the modified MSHIM. This is because the AO control system is blocked by the blocking signal from M-banks control system, and the blocking signal is unlocked quicker in the modified condition. And from Figure 9(b), it can be seen that the AO crossed the upper boundary at 3 points because the AO-bank control system is blocked from moving during the movement of M-banks. From Table 2, it can be seen that, after the modification of the power control system, I_P has been reduced by 87.4% from 196.27 to 24.72, which is a significant improvement. The drop of I_P means that the amplitude of big power mismatches and time are reduced, and, at the same time, the response speed of the control system is improved. Meanwhile, the overshoot of the signal and its steady-state errors are also reduced. M-Steps increased by 7.0% in the modified control system. Compared to the original control system, the modified control system has little sensitivity to control AO and to move the AO-bank, the same as to the max F_z.

This condition shows that the modified control system can control the core power and the axial power offset well in the 5% FP ramp load decrease. However, such improvement is based on the trade-off to increase the motion of the control rods.

Condition 2. The 10% FP step load decrease simulation results of the original and modified control strategy are shown in Figure 10 and Table 3.

Figure 10 shows that the core power and AO are well regulated during the typical 10% FP step load decrease. Figure 10(a) shows that the overshoots of the two control strategies are almost the same, but the regulation time and steady-state error of the modified control strategy are smaller than those of the original one. That is because the P-controller decreases the response time and the steady-state error of the M-banks control system. For the same reason, as Condition 1,

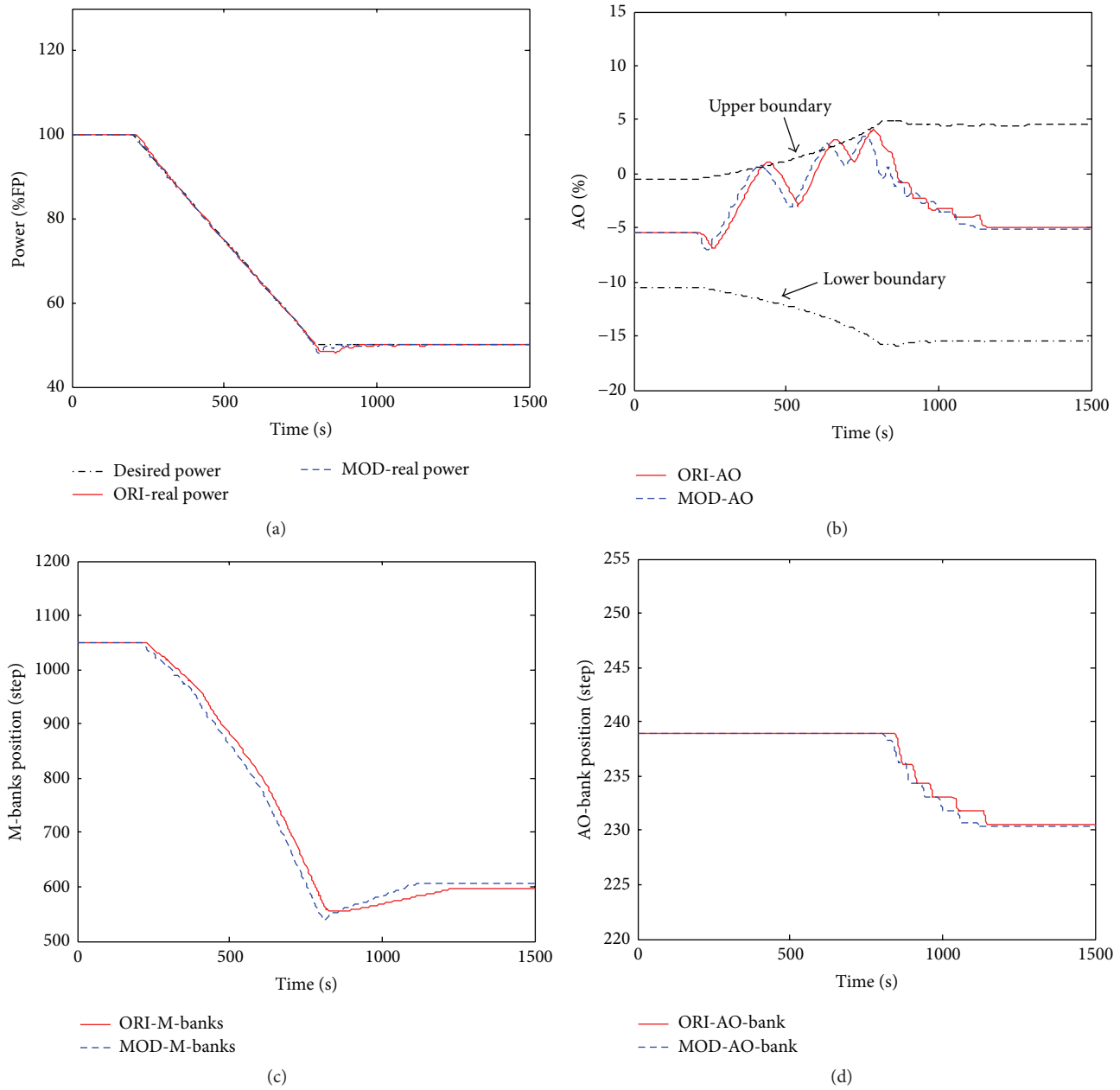

Figure 9: The 5% FP/min ramp load decrease simulation results obtained with the improved MSHIM control strategy: (a) desired and real nuclear powers (% FP), (b) AO (%), (c) M-bank position (Step), and (d) AO-bank position (Step) (the prefixes "ORI-" and "MOD-" denote the "original" and "modified," resp.).

the modified MSHIM makes the AO changing faster as shown in Figures 10(b) and 10(d). Table 3 shows the performance indices comparison of the two control strategies. After the modification of the power control system, I_P has been reduced by 55.8% from 257.04 to 113.70. The drop of I_P means that the amplitude of big power mismatches and time are reduced. Taken together, the movement steps of the M-banks were increased by 12.5% in the modified control system. The changes of I_{AO}, AO-Steps, and F_z by the modified control system are little.

Table 3: Five performance indices from the 10% FP step load decrease simulation of the original and modified power control system in MSHIM.

Performance indices	I_P	I_{AO}	F_z	M-Steps	AO-Steps
Original	257.04	3.02	1.1590	152	7
Modified	113.70	3.20	1.1571	171	7

This condition shows that, based on the trade-off to increase the motion of the control rods, the modified control

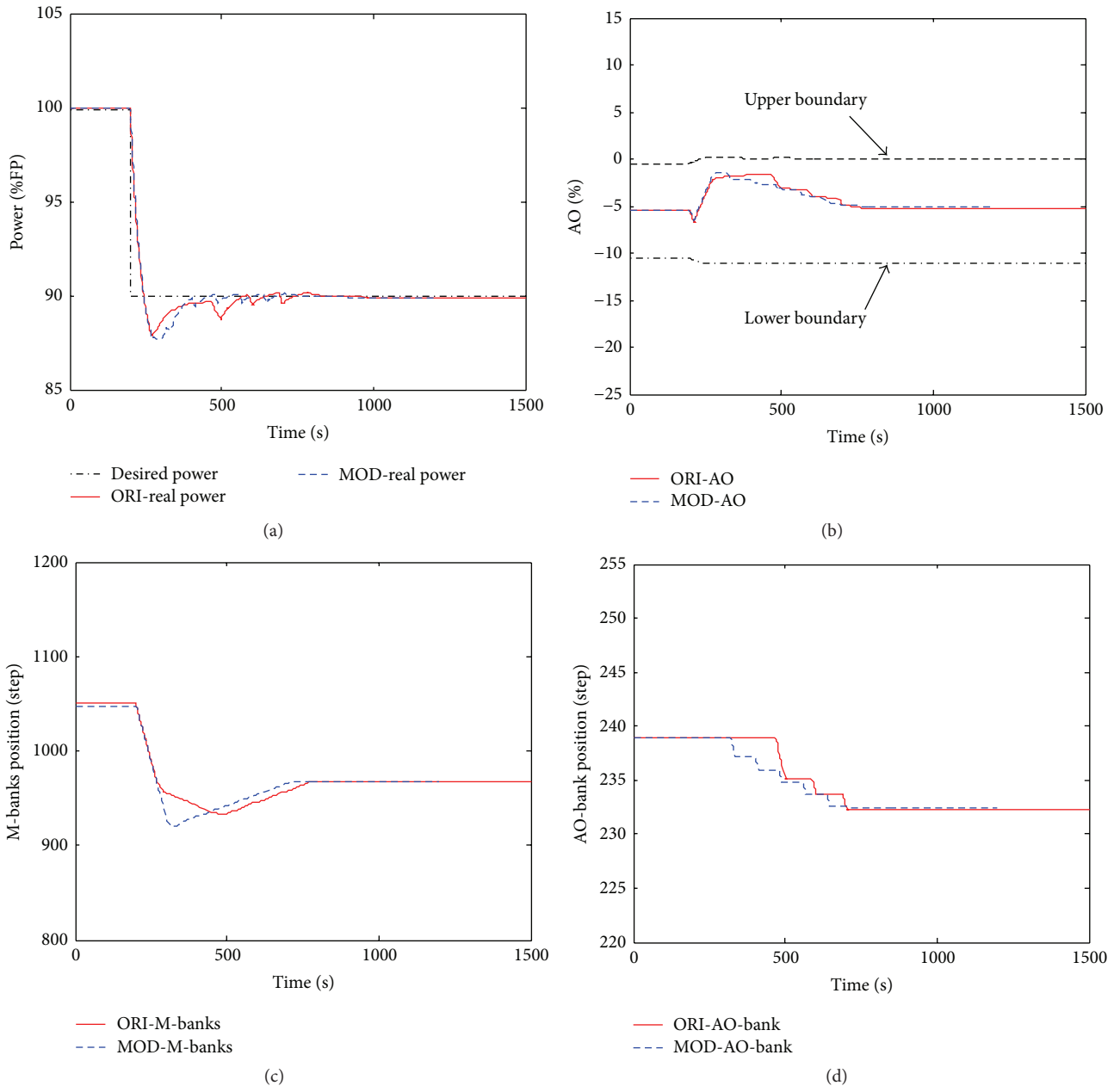

Figure 10: The 10% FP step load decrease simulation results obtained with the improved MSHIM control strategy: (a) desired and real nuclear powers (%FP), (b) AO (%), (c) M-bank position (Step), and (d) AO-bank position (Step).

system can control the core power and the axial power offset well in the 10% FP step load decrease.

Condition 3. The load follow simulation results of the original and modified control strategy are shown in Figure 11 and Table 4.

From Figure 11, it can be seen that the core power follows the target well for both original and modified MSHIM. And AO is restrained strictly between the upper and lower boundaries. Meanwhile, the power difference controlled by the two control strategies is very small, and the AO is controlled more strictly by the original control strategy. This is because the M-banks move more frequently in the modified strategy, leading

Table 4: Five performance indices from the load follow simulation of the original and modified power control system in MSHIM.

Performance indices	I_P	I_{AO}	F_z	M-Steps	AO-Steps
Original	233.81	12.88	1.1431	2477	352
Modified	135.18	9.94	1.1447	3073	416

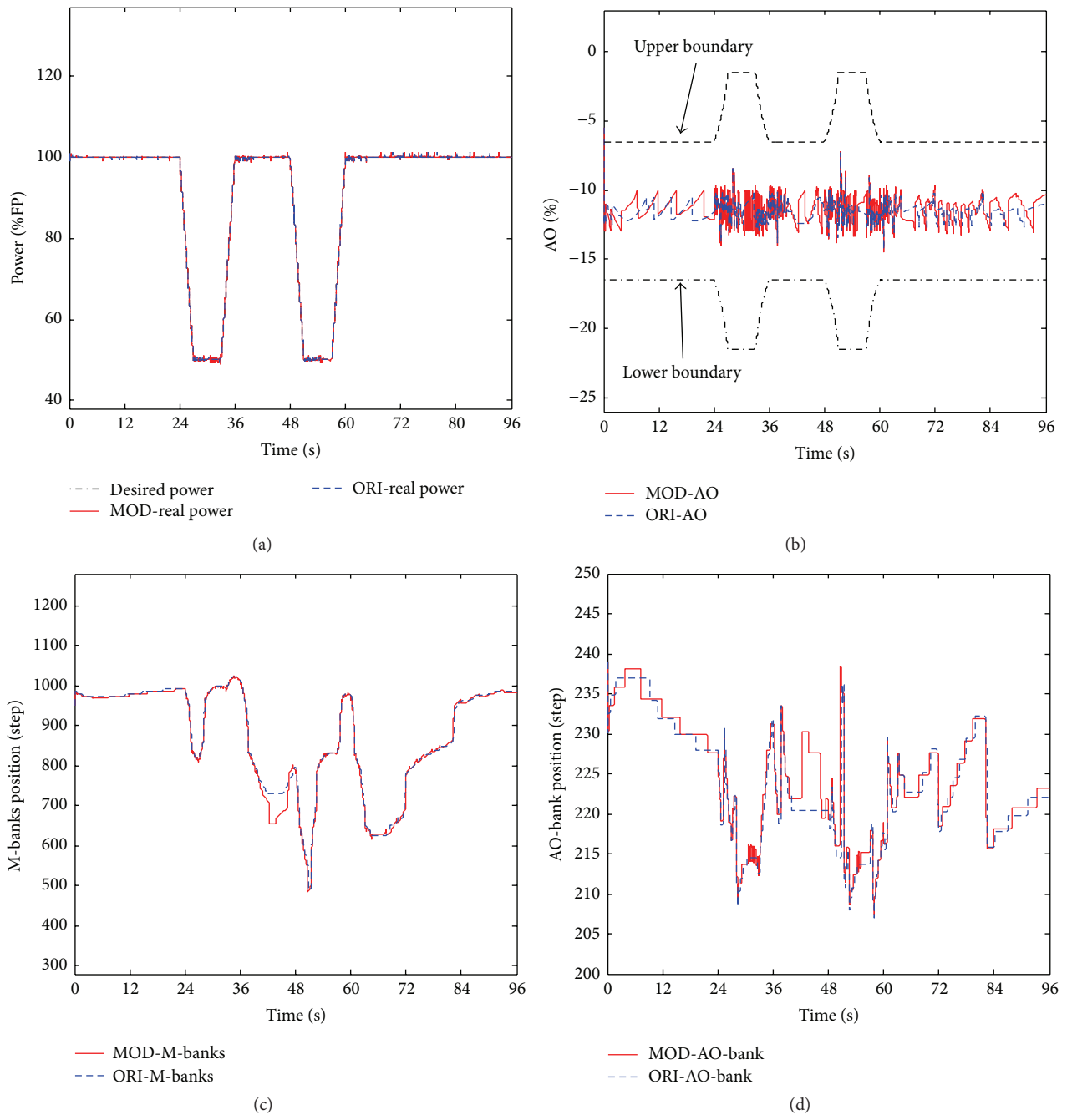

FIGURE 11: The load follow simulation results obtained with the improved MSHIM control strategy: (a) desired and real nuclear powers (%FP), (b) AO (%), (c) M-bank position (Step), and (d) AO-bank position (Step).

to the blocking of the AO-bank. From Table 4, I_P reduces by 42.2% from 233.81 to 135.18; taken together, M-Steps increase by 24.1% from 2477 to 3073. Different from the former two conditions, the changes of I_{AO} and AO-Steps are obvious. I_{AO} reduces by 22.8%, and AO-Steps increase by 18.2%. Comparing to Conditions 1 and 2, it is clear that the decrease of I_P is smaller and the increases of I_{AO}, M-Steps, and AO-Steps are greater. This is mainly because the xenon iodine dynamics are obvious in this long term power cycle of Condition 3.

5. Conclusion

In this paper, a modified MSHIM control system is introduced and verified by theoretical and simulation analysis. In the new control system, the coolant average temperature error signal is used to control the power level in the reactor core. The proposed method has been verified by dynamic performance simulation and compared to the original control system. The calculation results showed that the modified

control system has simplified the control logic and enhanced the control performance at the same time.

Nomenclature

C: Relative concentration of the delayed neutron precursor
D: Diffusion coefficient
d: Center distance of the neighboring nodes
e_P: Difference between the relative power and the target power
e_{AO}: Difference between the real and target AO
F_z: Power peak factor
f_f: Fraction of the core power generated in the fuel
G: Control component
I: Relative concentrations of iodine
I_P: Squared integral of the relative power mismatch
I_{AO}: Squared integral of the AO mismatch
K_{QT}: Variable gain
K_n: Nonlinear gain
M: Product of mass flow rate and the heat capacity of the coolant
N: Relative neutron concentration
P: Power
T: Temperatures
X: Relative concentrations of xenon.

Greek Symbols

α: Reactivity coefficients
β: Fraction of the delayed neutron group
γ: Fission yields
ΔH: Node height
Λ: Average neutron generation time
λ: Decay constant
μ: Heat capacities
ρ: Reactivity
σ: Microscopic cross section
τ: Time constant
ϕ: Neutron flux
Ω: Transfer coefficient between the fuel and coolant.

Subscripts

ave: Average value
err: Error
ref: Reference value
i: Node number
0: Steady-state value
f: Fuel
c: Coolant
I: Iodine
X: Xenon.

Conflict of Interests

The authors declare that there is no conflict of interests regarding the publication of this paper.

Acknowledgments

This work was supported by the National Science Foundation of China under Grant 11405125, China Postdoctoral Science Foundation Funded Project under Grant 2014M562420, and the Fundamental Research Funds for the Central Universities of China under Grant 2015gjhz09.

References

[1] Westinghouse Electric Company, *AP1000 Design Control Document*, Rev. 15, Westinghouse Electric Company, 2005.

[2] T. L. Schulz, "Westinghouse AP1000 advanced passive plant," *Nuclear Engineering and Design*, vol. 236, no. 14–16, pp. 1547–1557, 2006.

[3] Westinghouse Electric Company, AP1000 Fuel Design & Core Operations, 2010.

[4] M. Onoue, T. Kawanishi, and W. R. Carlson, "Application of MSHIM core control strategy for westinghouse AP1000 nuclear power plant," in *Proceedings of the International Conference on Global Environment and Advanced Nuclear Power Plants (GENES4/ANP '03)*, Kyoto, Japan, September 2003.

[5] K. J. Drudy, T. Morita, and B. T. Connelley, "Robustness of the MSHIM operation and control strategy in the AP1000 design (ICONE '17)," in *Proceedings of the 17th International Conference on Nuclear Engineering*, pp. 893–904, Brussels, Belgium, July 2009.

[6] R. J. Fetterman, "Advanced first core design for the Westinghouse AP1000," in *Proceedings of the 17th International Conference on Nuclear Engineering (ICONE '09)*, pp. 167–174, Brussels, Belgium, July 2009.

[7] L. Liu, L. Zheng, and F. Zhou, "Preliminary study on operational transient analysis for AP1000," *Nuclear Techniques*, vol. 35, no. 11, pp. 869–876, 2012.

[8] P. Wang, J. Wan, Z. Chen et al., "Dynamic simulation and study of Mechanical Shim (MSHIM) core control strategy for AP1000 reactor," *Annals of Nuclear Energy*, vol. 72, pp. 49–62, 2014.

[9] S. R. Shimjith, A. P. Tiwari, M. Naskar, and B. Bandyopadhyay, "Space-time kinetics modeling of Advanced Heavy Water Reactor for control studies," *Annals of Nuclear Energy*, vol. 37, no. 3, pp. 310–324, 2010.

[10] P. F. Wang, Y. Liu, B. T. Jiang, J. S. Wan, and F. Y. Zhao, "Nodal dynamics modeling of AP1000 reactor for control system design and simulation," *Annals of Nuclear Energy*, vol. 62, pp. 208–223, 2014.